Agonist activation of p42 and p44 mitogen-activated protein kinases following expression of the mouse δ opioid receptor in Rat-1 fibroblasts: effects of receptor expression levels and comparisons with G-protein activation

Andrew R. BURT*, I. Craig CARR*, Ian MULLANEY*, Neil G. ANDERSON† and Graeme MILLIGAN*‡

* Molecular Pharmacology Group, Division of Biochemistry and Molecular Biology, Institute of Biomedical and Life Sciences, University of Glasgow, Glasgow G12 8QQ, Scotland, U.K., and †Hannah Research Institute, Ayr KA6 5HL, Scotland, U.K.

Rat-1 fibroblasts were transfected with a cDNA encoding the mouse δ opioid receptor. Two separate clones, D2 (which expressed some 6 pmol of the receptor/mg of membrane protein) and DOE (which expressed some 0.2 pmol/mg of membrane protein), were examined in detail. With membranes from both clones, the opioid agonist [D-Ala^2]leucine enkephalin (DADLE) caused stimulation of high-affinity GTPase activity and of the binding of guanosine 5′-[γ-[^{35}S]thio]triphosphate, and inhibition of forskolin-amplified adenylate cyclase activity. DADLE also induced phosphorylation and activation of both the p42^{MAPK} (42 kDa isoform) and p44^{MAPK} (44 kDa isoform) members of the mitogen-activated protein kinase (MAP kinase) family. All of these effects of DADLE were prevented in both clones by pretreatment of the cells with pertussis toxin. The maximal response that could be produced by DADLE in direct assays of G-protein activation were substantially greater in clone D2 than in clone DOE, but in both clones essentially full phosphorylation of both p42^{MAPK} and p44^{MAPK} could be achieved. EC_{50} values for DADLE stimulation of GTPase activity and for activation of p44^{MAPK} were substantially lower in clone D2 than in clone DOE. Moreover, in both clones the EC_{50} value for DADLE stimulation of p44^{MAPK} was substantially lower than that for stimulation of GTPase activity, and the Hill coefficients for agonist activation of p44^{MAPK} ($h > 1$) displayed marked co-operativity whereas those for G-protein activation did not (h 0.8–1.0). DADLE activation of p44^{MAPK} showed more sustained kinetics in clone D2 than in clone DOE. By contrast, lysophosphatidic acid, acting at an endogenously expressed G-protein-coupled receptor, also activated p44^{MAPK} in both clones in a pertussis toxin-sensitive manner, but both the kinetics and the concentration–response curve for activation of p44^{MAPK} by this ligand were similar. As with other systems, maintained cellular levels of a cAMP analogue prevented the effects of both G-protein-coupled receptors on activation of p44^{MAPK}. These results demonstrate for the first time that an opioid receptor, at least when expressed in Rat-1 fibroblasts, is able to initiate activation of the MAP kinase cascade in a G_i-dependent manner, and show that only a very small proportion of the cellular G_i population is required to be activated to result in full phosphorylation of the p42^{MAPK} and p44^{MAPK} MAP kinases.

INTRODUCTION

A considerable number of G-protein-coupled receptors (GPCRs) have been shown in particular cell systems to be able to increase the phosphorylation state and activity of the p42^{MAPK} (42 kDa isoform) and p44^{MAPK} (44 kDa isoform) members of the mitogen-activated protein kinase (MAP kinase) family [1], an event that has been more traditionally associated with activation of the single-transmembrane-helix growth factor tyrosine kinase receptors [1]. Much of the initial work in this area utilized endogenously expressed receptors for lysophosphatidic acid (LPA) [2,3] and thrombin [4,5]. However, due to the lack of knowledge of the molecular structure of the LPA receptor and the very limited available pharmacology at both of these receptors [6], further work has also utilized cell systems transfected to express particular GPCRs [7–11]. We have previously transfected Rat-1 fibroblasts with the α_{2A}-adrenoceptor [7,12] and shown that, in this environment, agonist occupation of the receptor results in enhanced GTP loading of p21^{ras} and phosphorylation of both p42^{MAPK} and p44^{MAPK}. Both of these effects were blocked by pretreatment of the cells with concentrations of pertussis toxin sufficient to cause maximal ADP-ribosylation of the α subunit of the G_i-like G-proteins. Others have used related systems to implicate further components of the p21^{ras} pathway in these events and to show that elevation of intracellular cAMP levels can limit agonist-induced MAP kinase phosphorylation [12–17]. There is currently little information available, however, on the quantitative aspects of the extent to which GPCRs must be expressed in order to observe activation of the MAP kinase cascade, and how this relates to the degree of G-protein stimulation that can be achieved by a particular receptor.

In the present study we demonstrate that expression of the mouse δ opioid receptor [18–20] in Rat-1 fibroblasts allows agonist-mediated stimulation of p42^{MAPK} and p44^{MAPK}. We (1) examine the relative effectiveness of an agonist in clones of these cells expressing different levels of the receptor, (2) show that the clones display a large receptor reserve for agonist-induced activation of p42^{MAPK} and p44^{MAPK}, (3) demonstrate that this activation displays co-operativity in agonist concentration–effect curves, (4) is more sustained in cells expressing higher levels of the receptor, and (5) requires activation of only a small fraction of the cellular G_i population.

Abbreviations used: GPCR, G-protein-coupled receptor; MAP kinase, mitogen-activated protein kinase; p44^{MAPK} and p42^{MAPK}, 44 kDa and 42 kDa isoforms respectively of MAP kinase; LPA, lysophosphatidic acid; DADLE, [D-Ala^2]leucine enkephalin; RT-PCR, reverse transcriptase-PCR; GTP[S], guanosine 5′-[γ-thio]triphosphate; EGF, epidermal growth factor.

‡ To whom correspondence should be addressed.

MATERIALS AND METHODS

Materials

Guanosine 5′-[γ-[^{35}S]thio]triphosphate ([^{35}S]GTP[S]; 1026 Ci/mmol) and [^{32}P]NAD$^+$ (800 Ci/mmol) were obtained from DuPont/New England Nuclear. [γ-^{32}P]GTP (> 10 Ci/mmol), [γ-^{32}P]ATP (3000 Ci/mmol), [^{3}H]diprenorphine (50 Ci/mmol) and the Biotrak p42/p44 MAP kinase enzyme assay system were obtained from Amersham International. Cholera toxin was from Sigma and pertussis toxin was from Porton Products (Porton Down, Wilts., U.K.). All reagents for tissue culture were from Life Technologies (Paisley, Strathclyde, U.K.). Hygromycin B was from Boehringer Mannheim (Mannheim, Germany). Opioid ligands were from Research Biochemicals Inc., Torcis Cookson or Sigma. The cDNA encoding the mouse δ opioid receptor [20] was kindly donated by Dr. Graeme Bell, Howard Hughes Medical Institute, University of Chicago, Chicago, IL, U.S.A.

Generation and isolation of clones of Rat-1 fibroblasts expressing the mouse δ opioid receptor

A cDNA encoding the mouse δ opioid receptor [20] was ligated into plasmid pCMV-ms12. Rat-1 fibroblasts were co-transfected with this cDNA (5 μg) and with the plasmid pBABEhygro (0.5 μg), which is able to direct expression of the hygromycin B resistance marker, using Lipofectin reagent (Life Technologies) according to the manufacturer's instructions. Clones that demonstrated resistance to hygromycin B (200 μg/ml) were selected and expanded. Expression of the δ opioid receptor polypeptide in membranes from these clones was assessed initially by the specific binding of the opioid receptor ligand [^{3}H]diprenorphine (see the Results section) and detection of relevant mRNA using reverse transcriptase-PCR (RT-PCR) (results not shown; but see [21]).

Cell culture

Cells of clones D2 and DOE were grown in Dulbecco's modified Eagle's medium supplemented with 5% (v/v) donor calf serum, penicillin (100 units/ml) and streptomycin (100 μg/ml) in 5% CO_2 at 37 °C. Cells were grown in 75 cm^2 tissue culture flasks and were harvested just prior to confluency. In a number of cases, cells were treated with pertussis toxin (25 ng/ml) for 16 h prior to cell harvest. Membranes were prepared from the cells by homogenization with a Teflon-on-glass homogenizer and differential centrifugation as described for a variety of other cells [22].

[^{3}H]Diprenorphine binding experiments

In experiments designed to define ligand specificity, membranes from clones D2 and DOE (10 μg) were incubated at 30 °C for 45 min in 20 mM Tris/HCl (pH 7.5), 50 mM sucrose and 20 mM $MgCl_2$ (buffer A) containing 10 nM [^{3}H]diprenorphine in the absence and presence of 10 μM [D-Ala^2]leucine enkephalin (DADLE) to define maximal and non-specific binding respectively of the δ opioid receptor. Specific binding, defined as above, represented more than 80% of the total binding of radioligand. The radioligand was competed by addition of various concentrations of each of DADLE, DSLET ([D-Ser^2]leucine enkephalin-Thr), DAMGO (H_2N-Tyr-D-Ala-Gly-*N*-Me-Phe-Gly-ol) and U-50488 {*trans*-(±)-3,4-dichloro-*N*-methyl-*N*-[2-(1-pyrrolidinyl)-cyclohexyl]benzeneacetamide}, compounds that show selectivity for the various opioid receptor subtypes (δ, μ and κ). These experiments confirmed the pharmacology of the expressed receptor as a δ opioid receptor (results not shown, but see [21]). All binding experiments were terminated by rapid filtration through Whatman GF/C filters followed by three washes (5 ml) with ice-cold buffer A. Filters were maintained overnight in 10 ml of Ultima-Flo AF scintillant before liquid scintillation counting.

RNA extraction

Total RNA was extracted from cells according to the acid phenol/guanidinium thiocyanate method of Chomczynski and Sacchi [23] using RNAzol B (Biogenesis). Purity and quantification of RNA were assessed by A_{260}/A_{280} ratios.

RT-PCR procedure

The RT-PCR procedure was carried out as follows. Samples of 5 μg of RNA (8 μl) were denatured by incubation at 65 °C for 10 min, chilled on ice and reverse-transcribed in 33 μl of reaction mixture using a first-strand cDNA synthesis kit (Pharmacia LKB Biotechnology) as detailed by the manufacturer. Incubation was carried out at 37 °C for 1 h and the reaction was stopped by heating samples at 95 °C for 5 min and then chilling on ice.

PCR reactions on the reverse-transcribed samples or on 200 ng of appropriate cDNA species were carried out using the following primers: mouse δ sense, 5′ GCTGTGCAAGGCTGTGCTCT 3′; mouse δ antisense, 5′ CCAGACGATGACGAAGATGTG 3′. Amplifications were performed in 100 μl of buffer containing 20–40 pmol of primers and 2.5 units of *Taq* polymerase (Promega) in a HYBAID Omnigene temperature cycler. Cycles were as follows: 95 °C/5 min, 55 °C/1 min, 72 °C/1 min (one cycle); 95 °C/30 s, 55 °C/1 min, 72 °C/1 min (30 cycles); 95 °C/30 s, 55 °C/1 min, 72 °C/5 min (one cycle). Reaction products were separated by 1.5–1.75% agarose gel electrophoresis. These experiments confirmed the expression of mRNA encoding the δ opioid receptor in both clones D2 and DOE, but not in parental Rat-1 fibroblasts (results not shown).

High-affinity GTPase assays

These were performed essentially as described in [24] using [γ-^{32}P]GTP (0.5 μM; 60000 c.p.m.) and various concentrations of DADLE. Non-specific GTPase activity was assessed by parallel assays containing 100 μM GTP.

[^{35}S]GTP[S] binding studies

These were performed as described in [25]. Briefly, membranes were incubated at 4 °C for 1 h in a final assay volume of 100 μl in a reaction mixture comprising 50 mM triethanolamine hydrochloride (pH 7.4), 5 mM $MgCl_2$, 1 mM EDTA, 1 mM dithiothreitol, 150 mM NaCl, 100 μM GDP and 0.3–0.5 nM [^{35}S]GTP[S] (50 nCi) in the presence or absence of ligand as described in the Results section. The incubation was terminated by the addition of 2.5 ml of ice-cold washing buffer B (50 mM Tris/HCl, pH 7.5, 5 mM $MgCl_2$) and rapid filtration through Whatman GF/C filters followed by three washes (5 ml) with ice-cold buffer B. Filters were maintained overnight in 10 ml of Ultima-Flo AF scintillant before liquid scintillation counting.

Agonist regulation of cholera toxin-catalysed [^{32}P]ADP-ribosylation

[^{32}P]ADP-ribosylation of membranes of cells of clones D2 and DOE was performed in the absence of added guanine nucleotides basically as in [26,27], except that sodium phosphate (pH 7.0) replaced potassium phosphate (pH 7.0). Further additions to the assays were as detailed in the Results section. Dried gels were exposed to a phosphor storage plate for 24 h and then analysed using a FUJIX BAS1000 image analyser.

Adenylate cyclase assays

These were performed as described in [28]. Separation of [^{32}P]ATP and [^{32}P]cAMP was achieved by the method of Salomon et al. [29].

Regulation of p42^{MAPK} and p44^{MAPK} phosphorylation/mobility and activity

The phosphorylation of p42^{MAPK} and p44^{MAPK} was determined by an electrophoretic mobility shift assay. Cells were stimulated with the appropriate ligand for various times (see the Results section for details) following maintenance in serum-free medium for 48 h, and subsequently lysed at 4 °C in a buffer containing 25 mM Tris/HCl, 40 mM *p*-nitrophenol, 25 mM NaCl, 10 % (v/v) ethylene glycol, 10 μM dithiothreitol, 0.2 % (v/v) Nonidet P40, 1 μg/ml aprotinin, 1 mM sodium orthovanadate, 3.5 μg/ml pepstatin A and 200 μM PMSF at pH 7.5. Following centrifugation of the lysed samples in a Microfuge (13000 rev./min, 5 min), SDS/PAGE loading buffer was added to a sample of the supernatant and applied to an SDS/PAGE gel [10 % (w/v) acrylamide, 0.063 % (w/v) bisacrylamide, containing 6 M urea] following heating of the sample in a boiling-water bath for 5 min [30]. Samples were transferred from the gel to nitrocellulose and immunoblotted with an anti-peptide antiserum raised against amino acids 325–345 of p44^{MAPK}, or with a monoclonal antibody that specifically recognizes p42^{MAPK}. These gel conditions provide excellent 'gel shift' of this polypeptide upon ligand regulation, a feature that is synonymous with its phosphorylation and activation [15]. The intensities of the phosphorylated and non-phosphorylated forms of p44^{MAPK} were assessed using a Bio-Rad model GS 670 imaging densitometer.

In a number of cases the activity state of p44^{MAPK} was assessed. Following stimulation as described above, cells were lysed at 4 °C in a buffer containing 20 mM Tris/HCl (pH 8), 137 mM NaCl, 1 mM EGTA, 1 % (v/v) Triton X-100, 10 % (v/v) glycerol, 3 mM $MgCl_2$, 100 μM orthovanadate, 25 mM NaF, 10μg/ml aprotinin and 200 μM PMSF, and MAP kinase activity was measured using the Biotrak p42/p44 MAP kinase enzyme assay system (Amersham International).

Data analysis

Analysis of data curves was performed using the Kaleidagraph curve-fitting package driven by an Apple Macintosh computer. All of the immunoblots displayed represent examples of at least three experiments performed on separate cell cultures.

RESULTS

Rat-1 fibroblast cells, which do not endogenously express an opioid receptor, were co-transfected in a 1:10 ratio with the plasmid pBABEhygro, which allows expression of resistance to hygromycin B, and plasmid pCMV-ms12, into which a cDNA encoding the mouse δ opioid receptor had been ligated [20]. Colonies displaying resistance to hygromycin B (200 μg/ml) were selected, expanded and examined for both mRNA corresponding to the δ opioid receptor by RT-PCR (results not shown, but see [21] for details) and expression of high-affinity binding sites for the opioid ligand [^{3}H]diprenorphine. Clone D2 expressed considerably higher levels (6400 $\pm$ 100 fmol/mg of membrane protein) of the δ opioid receptor than did clone DOE (170 $\pm$ 30 fmol/mg of membrane protein) (means $\pm$ S.E.M., $n = 3$ in each case).

In both of these clones the expressed δ opioid receptor was effectively coupled to the cellular G-protein signal transduction machinery, as shown by the ability of the opioid agonist DADLE to stimulate high-affinity GTPase activity. The maximal effect of DADLE in these assays was considerably greater in membranes of clone D2 than in those of clone DOE (Table 1), as anticipated from the higher level of receptor expression in the former clone. This coupling of the δ opioid receptor was predominantly, if not exclusively, to members of the G_i subfamily of G-proteins (Rat-1 cells express each of G_i1, G_i2 and G_i3 [31]), as indicated by the large decrease in the ability of DADLE to stimulate high-affinity GTPase activity in these membranes following pretreatment of the cells with pertussis toxin (Table 1). A further demonstration of the coupling of the expressed δ opioid receptor to the cellular G-protein population was obtained by measuring DADLE stimulation of the binding of [^{35}S]GTP[S] to membranes of both clones D2 and DOE. As with agonist stimulation of high-affinity GTPase activity, a substantially greater effect of DADLE was recorded in membranes of clone D2 (clone D2: basal binding, 72.1 $\pm$ 2.0 fmol/mg of membrane protein; 10 μM DADLE, 272.6 $\pm$ 7.3 fmol/mg; clone DOE: basal binding, 32.5 $\pm$ 1.6 fmol/mg; 10 μM DADLE, 49.1 $\pm$ 0.7 fmol/mg; means $\pm$ S.E.M., $n = 3$ in each case). Further proof of the functional interaction of the δ opioid receptor in these two clones with G_i-like G-proteins was the observation that DADLE was able to allow cholera toxin-catalysed [^{32}P]ADP-ribosylation of these proteins in membranes from each of these two clones (Figure 1). As anticipated

Table 1 DADLE stimulation of high-affinity GTPase activity in clone D2 is greater than in clone DOE and is prevented by pretreatment with pertussis toxin

High-affinity GTPase activity and its regulation by a maximally effective concentration of DADLE (10 μM) was measured as described in the Materials and methods section in membranes derived from cells of clones D2 and DOE, which were either untreated or pretreated with pertussis toxin (25 ng/ml, 16 h) prior to harvest of the cells. Data represent means $\pm$ S.E.M. from three independent experiments.

	High-affinity GTPase activity (pmol/min per mg of protein)	
Treatment	D2	DOE
Basal	23.3 $\pm$ 0.9	25.9 $\pm$ 0.7
DADLE	45.6 $\pm$ 2.1	32.4 $\pm$ 1.2
Pertussis toxin	12.5 $\pm$ 1.0	18.7 $\pm$ 1.1
Pertussis toxin + DADLE	12.4 $\pm$ 1.3	20.0 $\pm$ 0.4

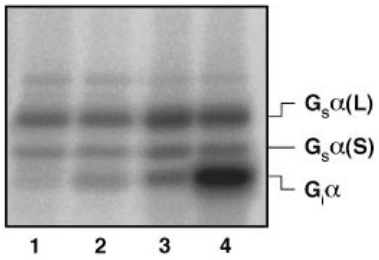

Figure 1 DADLE stimulation of cholera toxin-catalysed [^{32}P]ADP-ribosylation of the α subunit of G_i in clones D2 and DOE

Membranes (20 μg) of either clone DOE (lanes 1 and 2) or clone D2 (lanes 3 and 4) were subjected to cholera toxin-catalysed [^{32}P]ADP-ribosylation performed in the absence (lanes 1 and 3) or presence (lanes 2 and 4) of DADLE (10 μM), as described in the Materials and methods section. The autoradiograph shown is representative of those produced in four independent experiments. $G_s\alpha$(L) and $G_s\alpha$(S) are splice variants of $G_s\alpha$.

Table 2 DADLE-mediated inhibition of adenylate cyclase activity in membranes of clones D2 and DOE is attenuated by pretreatment with pertussis toxin

Adenylate cyclase activity and its regulation by ligands was measured as described in the Materials and methods section. Forskolin and DADLE were each present at 10 μM. Results are presented as means $\pm$ S.E.M., $n =$ 4 independent experiments. Values in parentheses are the percentage inhibition caused by DADLE.

	Adenylate cyclase activity (pmol/min per mg of protein)			
	Untreated		Pertussis toxin-treated	
	D2	DOE	D2	DOE
Basal	53.6 $\pm$ 2.8	99.6 $\pm$ 5.7	87.1 $\pm$ 3.9	119.6 $\pm$ 3.4
Forskolin	112.9 $\pm$ 2.6	175.8 $\pm$ 5.1	147.5 $\pm$ 4.0	167.7 $\pm$ 2.8
Forskolin + DADLE	91.9 $\pm$ 4.3 (35%)	155.6 $\pm$ 3.2 (27%)	145.7 $\pm$ 2.5 (3%)	172.0 $\pm$ 2.4 ($-$9%)

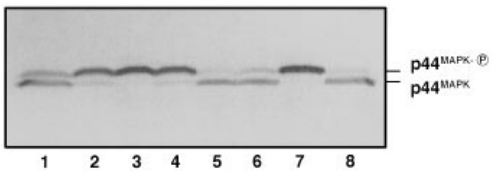

Figure 2 Pertussis toxin pretreatment of clone DOE cells prevents stimulation of p44^{MAPK} phosphorylation by DADLE and LPA, but not that by EGF

Clone DOE cells were deprived of serum for 48 h and then exposed to various agonists for 5 min. Some of these cells were treated with pertussis toxin (25 ng/ml; 16 h) prior to stimulation with agonists. The cells were lysed as described in the Materials and methods section, and fractions were resolved by SDS/PAGE and the phosphorylation state of p44^{MAPK} determined by immunoblotting. A representative immunoblot is shown for clone DOE cells treated with 1 μM DADLE (lanes 2 and 6), 10 nM EGF (lanes 3 and 7) or 10 μM LPA (lanes 4 and 8), or left unstimulated (lanes 1 and 5) for 5 min. Lanes 5–8 were pretreated with pertussis toxin; lanes 1–4 were not.

Table 3 EGF and DADLE increase MAP kinase activity in both clones D2 and DOE

MAP kinase activity was measured in cells of clones D2 and DOE as described in the Materials and methods section. Data are presented as means $\pm$ range from a representative experiment of two performed.

	MAP kinase activity (pmol/min per mg of protein)	
Condition	D2	DOE
Basal	242 $\pm$ 2	60 $\pm$ 1
DADLE (10 μM)	800 $\pm$ 10	416 $\pm$ 11
EGF (10 nM)	920 $\pm$ 20	600 $\pm$ 8

from the data decribed above, a considerably greater activation of the cellular G_i-like population was achieved with a maximally effective concentration of DADLE in clone D2 compared with clone DOE (Figure 1).

A functional output from the expressed δ opioid receptors in these clones was inhibition of forskolin-amplified adenylate cyclase activity, which was produced by DADLE in both clones (Table 2). A maximally effective concentration of DADLE (10 μM) was able to produce a somewhat greater inhibition of forskolin-stimulated adenylate cyclase in membranes from clone D2 (37.7 $\pm$ 7.5%; mean $\pm$ S.E.M., $n = 4$) than in those from clone DOE (24.6 $\pm$ 5.2%; $n = 5$). This signalling effect of the δ opioid receptor was also produced via activation of a G_i-like G-protein, as this effect of DADLE was attenuated following pertussis toxin treatment of the cells (Table 2).

Treatment of D2 or DOE cells with DADLE (1 μM for 5 min) led to phosphorylation of virtually the entire cellular population of both the p44 (Figure 2, and results not shown) and p42 (see below) members of the MAP kinase family, as assessed by the reduced mobility of these polypeptides through SDS/PAGE. A similar pattern was produced by treatment of these cells with either the tyrosine kinase receptor ligand epidermal growth factor (EGF) (10 nM) or LPA (10 μM), both of which have previously been reported to cause activation of these kinases in Rat-1 fibroblasts (e.g. see [7,12]) (Figure 2). Pertussis toxin pretreatment of both D2 and DOE cells prior to stimulation with the same ligands prevented the enhanced phosphorylation of p44^{MAPK} (Figure 2, and results not shown) produced by both DADLE and LPA, but did not alter the effect of EGF. Treatment of cells of clones D2 and DOE with DADLE (10 μM) or EGF (10 nM) also resulted in an enhancement of MAP kinase activity (Table 3). The basal MAP kinase activity was routinely noted to be higher in cells of clone D2 compared with clone DOE and, although the maximal MAP kinase activity that could be achieved in response to DADLE in clone D2 was higher than in clone DOE, this was also the case when stimulations were performed with EGF. The relative stimulation of MAP kinase activity by DADLE compared with that produced by EGF was similar in the two clones.

Concentration–response curves with DADLE indicated that considerably lower concentrations of this agonist were required to cause phosphorylation of p44^{MAPK} in clone D2 (Figures 3a and 3c) compared with clone DOE (Figures 3b and 3c) ($P = 0.04$), as assessed by the gel-shift assay. Half-maximal stimulation of phosphorylation of p44^{MAPK} was achieved with 0.073 $\pm$ 0.024 nM DADLE (mean $\pm$ S. E. M., $n = 3$) in cells of clone D2, whereas an approx. 40-fold higher concentration of this agonist was required to elicit the same effect in cells of clone DOE (EC_{50} = 3.1 $\pm$ 0.9 nM; $n = 4$). Direct measurements of MAP kinase activity also confirmed that substantially lower concentrations of DADLE were required to cause activation of MAP kinase in clone D2 compared with clone DOE (Figure 3d). Concentration–response curves for LPA stimulation of p44^{MAPK} phosphorylation in the two clones were, in contrast, not significantly different ($P = 0.11$) (clone D2, 0.12 $\pm$ 0.03 μM; clone DOE, 1.1 $\pm$ 0.5 μM; means $\pm$ S.E.M., $n = 3$ in each case) (Figure 4). Interestingly, the concentration–response curves both for DADLE-mediated p44^{MAPK} phosphorylation and for enhanced MAP kinase activity in both clones D2 and DOE were co-operative in nature, with

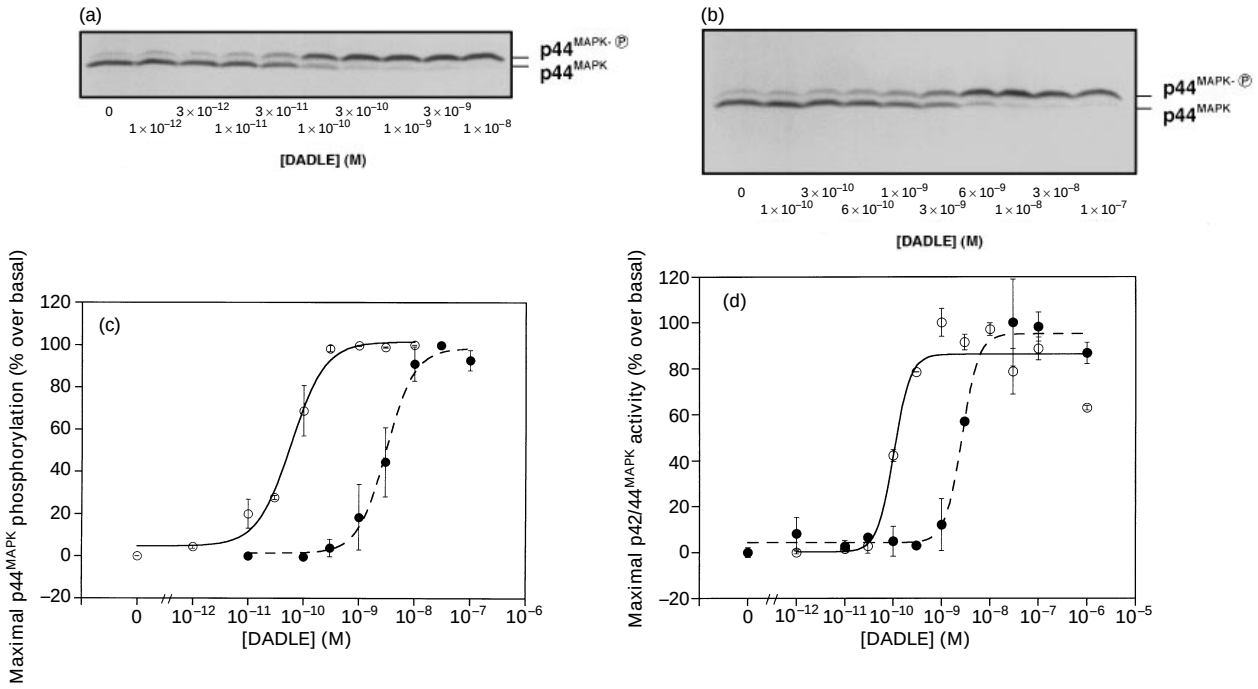

Figure 3 Concentration–response curves for DADLE-mediated phosphorylation of p44^{MAPK} in clones D2 and DOE

Cells of either clone D2 (**a**, and open symbols) or clone DOE (**b**, and closed symbols), deprived of serum for 48 h as described in the Materials and methods section, were exposed to various concentrations of DADLE for 5 min. The cells were lysed, and fractions were resolved by SDS/PAGE (**a–c**) and then immunoblotted to detect the presence and mobility of p44^{MAPK}. Decreased mobility of p44^{MAPK} is a reflection of its dual phosphorylation and activation. (**a**) Representative immunoblot of D2 cells; (**b**) representative immunoblot of DOE cells. The results in (**c**) were constructed following scanning of three pairs of immunoblots such as those in (**a**) and (**b**) and are means ± S.E.M. Direct MAP kinase activity measurements in cells of clones D2 and DOE are displayed in (**d**).

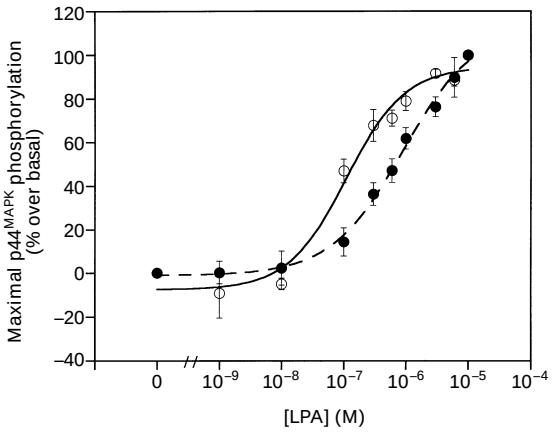

Figure 4 Concentration–response curves for LPA-mediated phosphorylation of p44^{MAPK} in clones D2 and DOE

Serum-starved D2 (○) and DOE (●) cells were stimulated with various concentrations of LPA for 5 min. Fractions of lysates of these cells were resolved by SDS/PAGE and immunoblotted for p44^{MAPK} as described in the Materials and methods section. The immunoblots were scanned and quantified as described in the legend to Figure 3. Data represent means ± S.E.M. from three independent experiments.

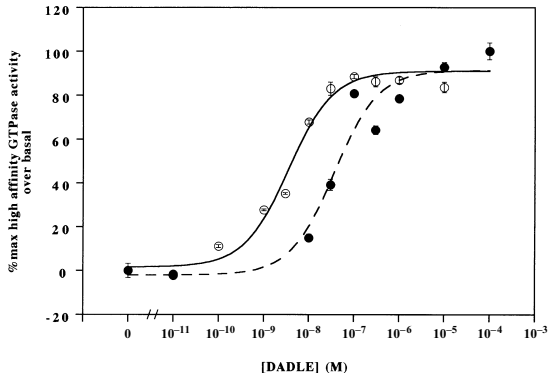

Figure 5 Concentration–response curves of DADLE-mediated stimulation of high-affinity GTPase activity in clones D2 and DOE

High-affinity GTPase activity was measured in membranes of clone D2 (○) and DOE (●) cells in the presence of various concentrations of DADLE. As the amount of stimulation produced by DADLE was higher in clone D2 than in clone DOE (see Table 1), results are presented as a percentage of the maximal effect of agonist (i.e. the effect produced in the presence of 0.1 mM DADLE), and were calculated as means ± S.E.M. ($n = 3$). In individual experiments with clone D2, basal GTPase activity varied between 22.5 and 23.7 pmol/min per mg of protein and the maximal effect of DADLE was between 49.6 and 52.8 pmol/min per mg of protein. In clone DOE, basal activity was between 13.6 and 21.7 pmol/min per mg of protein and that in the presence of DADLE was 20.9–28.6 pmol/min per mg of protein.

Hill coefficients (h) substantially greater than 1 (these varied between 1.4 and 3.0 in individual experiments) (Figure 3c). This was in contrast both to the effects of LPA on p44^{MAPK} phosphorylation (Figure 4) ($h = 0.75$–0.92) and to the concentration–effect curve for DADLE stimulation of high-affinity GTPase activity in these two clones (Figure 5), where $h = 0.8$–1.0.

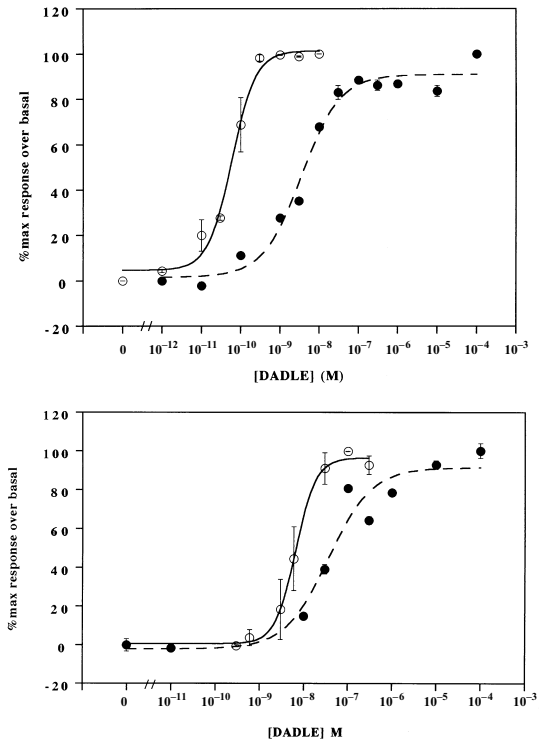

Figure 6 Comparisons of the stimulation by DADLE of high-affinity GTPase activity and the phosphorylation of p44^{MAPK} in clones D2 and DOE

Data from concentration–response curves with DADLE when measuring either phosphorylation of p44^{MAPK} (○) or stimulation of high-affinity GTPase activity (●) are presented for clone D2 (upper panel) and clone DOE (lower panel) as a percentage of the maximal effect produced by DADLE.

Concentration–response curves for DADLE stimulation of high-affinity GTPase activity in clones D2 and DOE also indicated a requirement for higher concentrations of DADLE to produce a half-maximal response in this measure of G-protein activation (EC_{50} values: D2, 5.7 ± 2.2 nM; DOE, 42 ± 6 nM) (Figure 5), but this was considerably less marked than for p44^{MAPK} phosphorylation. Direct comparison of the concentration–response curves for activation of p44^{MAPK} and stimulation of high-affinity GTPase activity demonstrated that only a very small fraction of the δ opioid receptor population (and thus only a small percentage of the cellular G_i population that can be activated by the receptor) of clone D2 cells was required to be occupied by agonist to cause maximal phosphorylation of p44^{MAPK}, indicating a very large receptor reserve in these cells for this function (Figure 6, upper panel). An obvious receptor and activated G_i protein reserve for p44^{MAPK} phosphorylation was also evident in clone DOE (Figure 6, lower panel), but this was considerably less ($P = 0.028$) than in clone D2 (compare the two panels of Figure 6).

The phosphorylation of p44^{MAPK} produced by addition of a maximally effective concentration of DADLE was more prolonged in duration in clone D2 than in clone DOE (Figures 7a–7c). This was also noted in direct MAP kinase activity assays (Figure 7d). In both clones, activation of p44^{MAPK} by DADLE was rapid and was easily detected within 1 min. In clone DOE maximal phosphorylation of these kinases was achieved at 5 min, but this was not maintained and by 15 min exposure to the ligand it had returned close to basal levels. By contrast, in clone D2 a high degree of activation of p44^{MAPK} in response to DADLE was observed for up to 30 min. The effect of LPA (10 μM) on the time course of p44^{MAPK} phosphorylation was not noticeably different in the two clones, being maximal following some 5 min exposure to the ligand and decaying thereafter such that levels of phosphorylation were greatly decreased within some 30–60 min (Figure 7e). The time courses of phosphorylation of p42^{MAPK} in response to DADLE in clones D2 and DOE were very similar to those for p44^{MAPK} (Figure 8).

Treatment of D2 and DOE cells with the cell-permeant analogue of cAMP, dibutyryl cAMP, prevented the ability of each of DADLE, LPA and EGF to cause p44^{MAPK} phosphorylation (Figure 9 and Table 4), as anticipated from previous studies.

DISCUSSION

Considerable progress has been made in recent times towards understanding the molecular components and interactions involved in coupling agonist occupation of certain GPCRs to enhanced phosphorylation and activation of the p44 and p42 members of the MAP kinase family of dually regulated kinases [1]. A key element in this cascade appears to be the $\beta\gamma$ complex of heterotrimeric G-proteins [8–10,32]. As the α subunits of the G_i-like G-proteins are often highly expressed in cells, then levels of $\beta\gamma$ complexes associated with these α subunits will also be high. This provides a potential rationale as to why many of the studies on MAP kinase regulation by GPCRs have utilized receptor species that interact with these G-proteins.

Despite the progress noted above, virtually nothing is known about the stoichiometry of this signalling process. In the present study we address this question by examining agonist regulation of the phosphorylation and activation of p44^{MAPK} and p42^{MAPK} in clones of Rat-1 fibroblasts expressing differing levels of the δ opioid receptor that we have isolated following transfection with a murine δ opioid receptor cDNA, and by comparing the effectiveness of this process with the ability of agonist occupation to cause activation of the cellular population of the G_i-like pertussis toxin-sensitive G-proteins.We have previously demonstrated in the genetic background of Rat-1 fibroblasts that the total cellular level of the α subunits of G_i-like G-proteins is in the region of 60 pmol/mg of membrane protein, with the bulk of this being contributed by $G_i2\alpha$ [31]. Functional interactions of the expressed δ opioid receptor with the cellular G-proteins in these two clones was defined by both agonist stimulation of high-affinity GTPase activity and stimulation of the binding of [^{35}S]GTP[S]. Both effects of the agonist were prevented in both cell lines by pretreatment with pertussis toxin, indicating that the relevant G-proteins are members of the G_i-like family. Further direct evidence for opioid receptor activation of G_i in these two clones was obtained in studies that examined agonist stimulation of [^{32}P]ADP-ribosylation of the G_i-like G-proteins catalysed by thiol-activated cholera toxin. This assay provides a diagnostic detection only of G-proteins activated by a receptor ligand (see [26,27] for examples and a theoretical basis).

In each of these assays, substantially greater G-protein activation was evident in clone D2 than in clone DOE, consistent with the greater levels of receptor expression in the former and with the G-protein population not being a limiting factor for cellular information transfer. By contrast with the markedly greater levels of G-protein activation achieved by the agonist DADLE in clone D2 compared with clone DOE, differences in the degree of maximal inhibition of forskolin-amplified adenylate cyclase were less pronounced in membranes from the two clones.

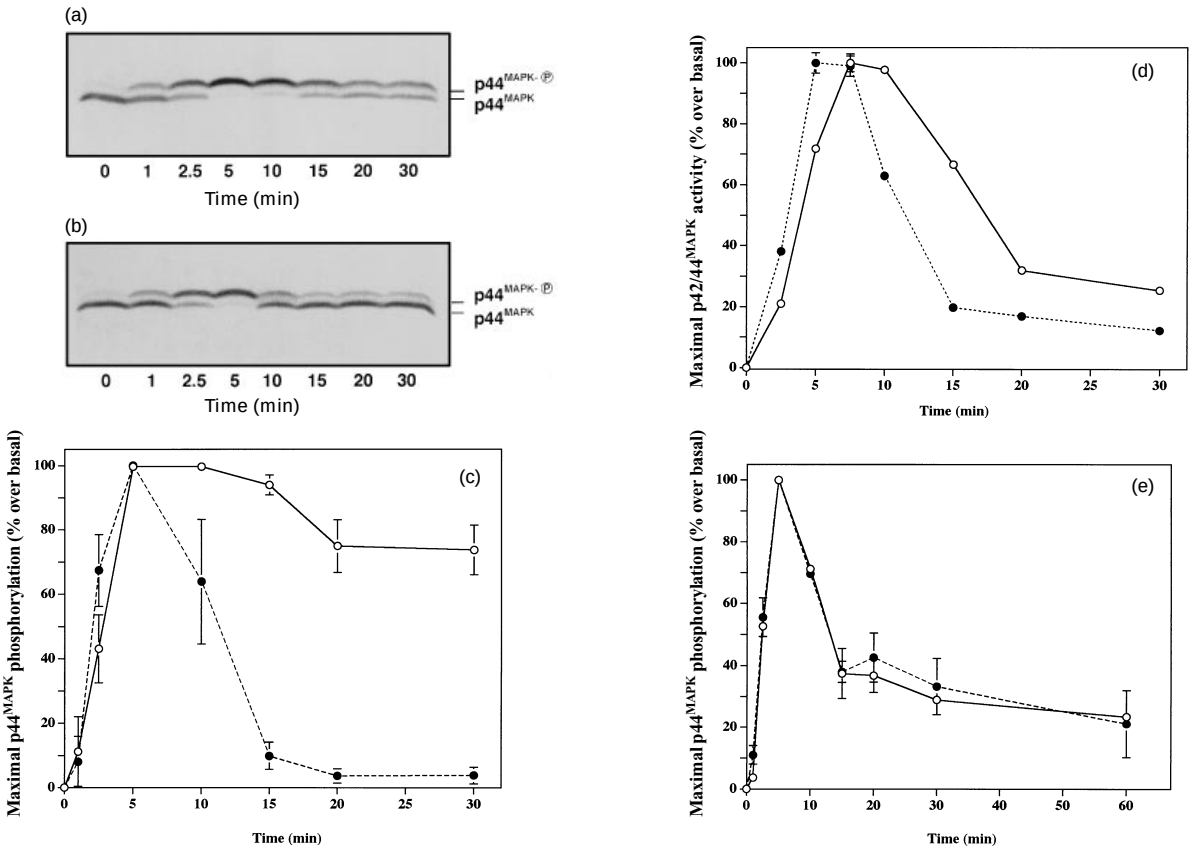

Figure 7 Prolonged phosphorylation of p44^{MAPK} by DADLE but not by LPA in clone D2 compared with clone DOE

Cells of clone D2 (**a**, **c**–**e**) or clone DOE (**b**, **c**–**e**) were exposed to DADLE (10 μM) (**a**–**d**) or LPA (10 μM) (**e**) for various times. Samples were then processed and p44^{MAPK} mobility/phosphorylation assessed (**a**–**c**, **e**). Representative p44^{MAPK} immunoblots of samples derived from cells of clone D2 (**a**) and clone DOE (**b**) are shown. Data from immunoblots such as those shown were scanned and the data are presented in (**c**) as the percentage of p44^{MAPK} in the phosphorylated state at differing times in clones D2 (○) and DOE (●). Data are presented as means ± S.E.M. ($n = 6$ for clone D2 and $n = 3$ for clone DOE). (**d**) MAP kinase activity measurements (means ± range) in clones D2 (○) and DOE (●). (**e**) Cells of clones D2 (○) and DOE (●) were exposed to LPA (10 μM) for various times and samples analysed as in (**a**)–(**c**). Data represent means ± range from $n = 2$ independent experiments.

Such data tend to implicate the adenylate cyclase catalytic element as the limiting component in this cascade in these cells. In both D2 and DOE cells, addition of DADLE resulted in maximal phosphorylation of both p44^{MAPK} and p42^{MAPK}, as determined by the decreased mobilities of these polypeptides through SDS/PAGE. These effects were also attenuated by pretreatment of the cells with pertussis toxin, whereas the stimulation of p44^{MAPK} phosphorylation in response to EGF was, as anticipated, unaffected by this manipulation.

Comparisons of the concentration–response curves for stimulation of GTPase activity and for MAP kinase phosphorylation and activation by DADLE in clones D2 and DOE revealed two novel and interesting features. Firstly, in both clones the Hill coefficient for DADLE-induced p44^{MAPK} phosphorylation was substantially greater than 1, thus indicating marked co-operativity. By contrast the Hill coefficients for agonist stimulation of high-affinity GTPase activity were close to 1. Interestingly, but perhaps rather surprisingly given the shape of the concentration–response curves with DADLE, phosphorylation of p44^{MAPK} in these clones in response to LPA did not show this feature of co-operativity (Figure 4). The receptor for LPA, although it has not been identified at a molecular level [33], is believed to be a GPCR, as effects of this lysophospholipid in Rat-1 fibroblasts have been demonstrated to be blocked by pertussis toxin treatment [2], and this agent has also been shown to activate G_i and to stimulate high-affinity GTPase activity [34]. It will be interesting to explore these differences more fully when the molecular structure of the LPA receptor becomes known. Secondly, the difference in the EC_{50} values for DADLE stimulation of p44^{MAPK} phosphorylation (0.073 nM) and for stimulation of high-affinity GTPase activity (5.7 nM) was some 80-fold in the high-receptor-expressing clone D2, whereas in clone DOE this difference for DADLE stimulation of p44^{MAPK} phosphorylation (3.1 nM) and for stimulation of high-affinity GTPase activity (42 nM) was only some 15-fold. These observations indicate both that there is a large reserve of the δ opioid receptor for MAP kinase phosphorylation in both of these clones (more so in clone D2) and that only a very small fraction of the cellular G_i-like G-protein population is required to be activated by the receptor to result in maximal phosphorylation of these MAP kinases. This may be relevant to why we routinely observed a degree of phosphorylation of p44^{MAPK} and p42^{MAPK} and higher MAP kinase activity in the absence of the opioid agonist following serum starvation of clone D2, while this was not obvious in clone DOE. δ Opioid and other GPCRs display differing degrees of spontaneous, empty-receptor, signal generation [21,35–38], and the higher levels of expression of the δ opioid receptor in clone D2 cells compared with clone DOE may be sufficient to produce

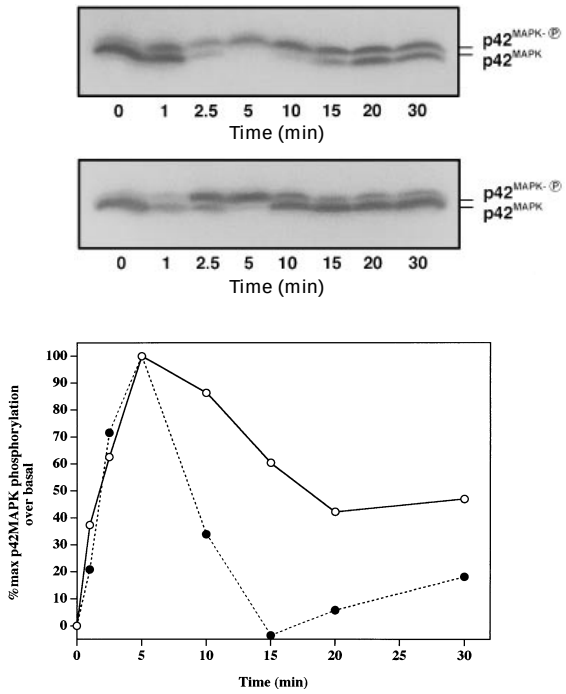

Figure 8 Time courses of phosphorylation of p42^{MAPK} by DADLE in clones D2 and DOE

Cells of clone D2 (top and bottom panels) or clone DOE (middle and bottom panels) were exposed to DADLE (10 μM) for various times. Samples were then processed and p42^{MAPK} mobility/phosphorylation assessed. Representative p42^{MAPK} immunoblots of samples derived from cells of clone D2 (top panel) and clone DOE (middle panel) are shown. The immunoblots displayed were scanned and the data are presented in the bottom panel as the percentage of p42^{MAPK} in the phosphorylated state at differing times in clones D2 (○) and DOE (●).

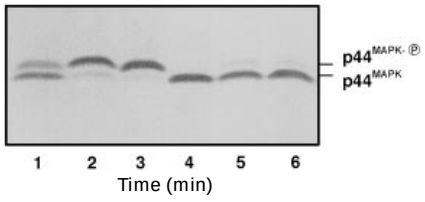

Figure 9 Dibutyryl cAMP attenuates DADLE stimulation of p44^{MAPK} phosphorylation in DOE cells

A representative immunoblot is shown for DOE cells unstimulated (lanes 1 and 4) or stimulated with 1 μM DADLE (lanes 2 and 5) or 10 nM EGF (lanes 3 and 6), after pretreatment with dibutyryl cAMP (1 mM, 20 min) (lanes 4–6) or with carrier only (lanes 1–3).

enough G-protein activation in the absence of agonist to result in measurable basal phosphorylation of the MAP kinases.

MAP kinase phosphorylation has been reported by a number of laboratories to be inhibited in the presence of maintained elevated concentrations of cAMP [14,16,17,39,40]. Addition of the membrane-permeant analogue of cAMP, dibutyryl cAMP, to clone D2 or clone DOE was sufficient to attenuate DADLE activation of p44^{MAPK} phosphorylation. DADLE was also able to inhibit adenylate cyclase activity in both clones (Table 2). Thus part of the observed co-operativity of DADLE activation of p44^{MAPK} phosphorylation may result from a combination of the agonist-induced decrease in cellular cAMP levels and the direct effects of the subunits of the activated G-protein with elements of

Table 4 Dibutyryl cAMP attenuates DADLE stimulation of p44^{MAPK} phosphorylation in clone D2

Serum-starved cells of clone D2 were stimulated with various agonists for 5 min after 20 min of pretreatment with or without 1 mM dibutyryl cAMP (dbcAMP). Cells were lysed and the phosphorylation status of p44^{MAPK} was determined by immunoblotting after SDS/PAGE as described in the Materials and methods section. Data represent means ± S.E.M. from three independent experiments.

	p44^{MAPK} in phosphorylated state (%)	
	−dbcAMP	+dbcAMP
Control	16.9 ± 7.2	0.3 ± 0.3
DADLE (10 μM)	92.7 ± 3.1	23.0 ± 11.2
EGF (10 nM)	98.0 ± 1.4	16.1 ± 17.2

the MAP kinase cascade upstream of p42^{MAPK} and p44^{MAPK}. This is purely speculation at this point; however, a related dual effect of a β-adrenoceptor on MAP kinase activity has been suggested by Crespo et al. [41].

Since the kinetics of the phosphorylation state of p44^{MAPK} in response to LPA were not different in clones D2 and DOE (Figure 7d), then the differences noted in the kinetics of sustained phosphorylation of the MAP kinases in the clones in response to DADLE (Figure 7c) must clearly be related to the levels of expression of the δ opioid receptor. The greater level of G-protein activation that can be obtained by maximally effective concentrations of DADLE in clone D2 compared with clone DOE was clearly demonstrated by the greater stimulation of high-affinity GTPase activity in membranes derived from the former, and more graphically by the markedly greater degree of DADLE-induced, cholera toxin-catalysed, [^{32}P]ADP-ribosylation of $G_i\alpha$ in membranes of clone D2 compared with clone DOE (Figure 1). As a sustained period of activation of this cascade seems to be reflected in greater mitogenic potential [42,43], it will be interesting, in time, to explore whether levels of G-protein activation produced by various partial agonists at a defined receptor will result in marked differences in either the maximal activation or the phosphorylation maintenance kinetics of the MAP kinases.

The studies reported herein extend our knowledge of the range of GPCRs that are able to interface with the MAP kinase cascade. Given the current understanding of a key role for G-protein $\beta\gamma$ subunits in this process, it was not entirely unexpected that the δ opioid receptor would be able to cause activation of p42^{MAPK} and p44^{MAPK}. However, for the first time we have provided data on how the degree and the kinetics of activation can vary in clones expressing differing levels of a GPCR, and we have shown that only a small fraction of the G-protein population available to a GPCR is required to be activated to cause maximal phosphorylation of p42^{MAPK} and p44^{MAPK}.

These studies were supported by the Biotechnology and Biological Sciences Research Council. A. R. B. thanks the BBSRC for a studentship. We thank Dr. Graeme Bell (Howard Hughes Medical Institute, University of Chicago, Chicago, IL, U.S.A.) for the gift of the cDNA encoding the mouse δ opioid receptor.

REFERENCES

1 Malarkey, K., Belham, C. M., Paul, A., Graham, A., McLees, A., Scott, P. H. and Plevin, R. (1995) Biochem. J. **309**, 361–375
2 van Corven, E. J., Hordijk, P. L., Medema, R. H., Bos, J. L. and Moolenaar, W. H. (1993) Proc. Natl. Acad. Sci. U.S.A. **90**, 1257–1261
3 Hordijk, P. L., Verlaan, I., van Corven, E. J. and Moolenaar, W. H. (1994) J. Biol. Chem. **269**, 645–651

4 L'Allemain, G., Pouyssegur, J. and Weber, M. J. (1991) Cell. Regul. **2**, 675–684
5 Kahan, C., Seuwen, K., Meloche, S. and Poussegur, J. (1992) J. Biol. Chem. **267**, 13369–13375
6 Moolenaar, W. H. (1995) J. Biol. Chem. **270**, 12949–12952
7 Alblas, J., van Corven, E. J., Hordijk, P. L., Milligan, G. and Moolenaar, W. H. (1993) J. Biol. Chem. **268**, 22235–22238
8 Koch, W. J., Hawes, B. E., Allen, L. F. and Lefkowitz, R. J. (1994) Proc. Natl. Acad. Sci. U.S.A. **91**, 12706–12710
9 Crespo, P., Xu, N., Simonds, W. F. and Gutkind, J. S. (1994) Nature (London) **369**, 418–420
10 Faure, M., Voyno-Yasenetskaya, T. A. and Bourne, H. R. (1994) J. Biol. Chem. **269**, 7851–7854
11 Winitz, S., Russell, M., Qian, N.-X., Dwyer, L. and Johnson, G. L. (1993) J. Biol. Chem. **268**, 19196–19199
12 Anderson, N. G. and Milligan, G. (1994) Biochem. Biophys. Res. Commun. **200**, 1529–1535
13 Cook, S. J., Rubinfeld, B., Albert, I. and McCormick, F. (1993) EMBO J. **12**, 3475–3485
14 Hordijk, P. L., Verlaan, I., Jalink, K., van Corven, E. J. and Moolenaar, W. H. (1994) J. Biol. Chem. **269**, 3534–3538
15 Howe, L. R. and Marshall, C. J. (1993) J. Biol. Chem. **268**, 20717–20720
16 Sevetson, B. R., Kong, X. and Lawrence, Jr., J. C. (1993) Proc. Natl. Sci. U.S.A. **90**, 10305–10309
17 Cook, S. J. and McCormick, F. (1993) Science **262**, 1069–1072
18 Kieffer, B., Befort, K., Gaveriaux-Ruff, C. and Hirth, C. G. (1992) Proc. Natl. Acad. Sci. U.S.A. **89**, 12048–12052
19 Evans, C. J., Keith, Jr., D. E., Morrison, H., Magendzo, K. and Edwards, R. H. (1992) Science **258**, 1952–1955
20 Yasuda, K., Raynor, K., Kong, H., Breder, C. D., Takeda, J., Reisine, T. and Bell, G. I. (1993) Proc. Natl. Acad. Sci. U.S.A. **90**, 6736–6740
21 Mullaney, I., Carr, I. C. and Milligan, G. (1996) Biochem. J. **315**, 227–234
22 Milligan, G. (1987) Biochem. J. **245**, 501–505
23 Chomczynski, P. and Sacchi, N. (1987) Anal. Biochem. **162**, 156–159
24 Koski, G. and Klee, W. A. (1981) Proc. Natl. Acad. Sci. U.S.A. **78**, 4185–4189
25 Wieland, T. and Jakobs, K. H. (1994) Methods Enzymol. **237**, 3–13
26 Milligan, G. and McKenzie, F. R. (1988) Biochem. J. **252**, 369–373
27 Milligan, G., Carr, C., Gould, G. W., Mullaney, I. and Lavan, B. E. (1991) J. Biol. Chem. **266**, 6447–6455
28 Milligan, G., Streaty, R. A., Gierschik, P., Spiegel, A. M. and Klee, W. A. (1987) J. Biol. Chem. **262**, 8626–8630
29 Salomon, Y., Londos, C. and Rodbell, M. (1974) Anal. Biochem. **58**, 541–548
30 Lee, T. W., Anderson, L. A., Eidne, K. A. and Milligan, G. (1995) Biochem. J. **310**, 291–298
31 McClue, S. J., Selzer, E., Freissmuth, M. and Milligan, G. (1992) Biochem. J. **284**, 565–568
32 van Biesen, T., Hawes, B. E., Luttrell, D. K., Krueger, K. M., Touhara, K., Porfiri, E., Sakaue, M., Luttrell, L. M. and Lefkowitz, R. J. (1995) Nature (London) **376**, 781–784
33 van der Bend, R. L., Brunner, J., Jalink, K., van Corven, E. J., Moolenaar, W. H. and van Blitterswijk, W. J. (1992) EMBO J. **11**, 2495–2501
34 Carr, C., Grassie, M. and Milligan, G. (1994) Biochem. J. **298**, 493–497
35 Chidiac, P., Hebert, T. E., Valiquette, M., Dennis, M. and Bouvier, M. (1994) Mol. Pharmacol. **45**, 490–499
36 Samama, P., Pei, G., Costa, T., Cotecchia, S. and Lefkowitz, R. J. (1994) Mol. Pharmacol. **45**, 390–394
37 Labrecque, J., Fargin, A., Bouvier, M., Chidiac, P. and Dennis, M. (1995) Mol. Pharmacol. **48**, 150–159
38 Barker, E. L., Westphal, R. S., Schmidt, D. and Sanders-Bush, E. (1994) J. Biol. Chem. **269**, 11887–11890
39 Wu, J., Dent, P., Jelinek, T., Wolfman, A., Weber, M. J. and Sturgill, T. W. (1993) Science **262**, 1065–1069
40 Graves, L. M., Bornfeld, K. E., Raines, E. W., Potts, B. C., MacDonald, S. G., Ross, R. and Krebs, E. G. (1993) Proc. Natl. Acad. Sci. U.S.A. **90**, 10300–10304
41 Crespo, P., Cachero, T. G., Xu, N. and Gutkind, J. S. (1995) J. Biol. Chem. **270**, 25259–25265
42 Meloche, S., Seuwen, K., Pages, G. and Pouyssegur, J. (1993) Mol. Endocrinol. **6**, 845–854
43 Marshall, C. J. (1995) Cell **80**, 179–185

Received 27 March 1996/27 June 1996; accepted 25 July 1996